Generation and Characterization of Urokinase Receptor-deficient Mice

Mieke Dewerchin,*‡ An Van Nuffelen,*‡ Goedele Wallays,* Ann Bouché,* Lieve Moons,* Peter Carmeliet,* Richard C. Mulligan,‡§ and D. Collen*

**Center for Transgene Technology and Gene Therapy, Vlaams Interuniversitair Instituut voor Biotechnologie, B-3000 Leuven, Belgium; and ‡Whitehead Institute for Biomedical Research and §Department of Biology, Massachusetts Institute of Technology, Cambridge, Massachusetts 02142*

Abstract

Mice homozygously deficient for the urokinase-type plasminogen activator (u-PA) receptor (*u-PAR*$^{-/-}$) were generated by homologous recombination in D_3 embryonic stem cells. The genomic sequences comprising exon 2 through 5 of the *u-PAR* gene were replaced by the *neomycin resistance* gene, resulting in inactivation of both *u-PAR* splice variants. The inactivated *u-PAR* allele was transmitted via mendelian inheritance, and *u-PAR*$^{-/-}$ mice displayed normal viability, growth, and fertility. Inactivation of *u-PAR* was confirmed by the absence of binding of rabbit anti–murine u-PAR or of an aminoterminal fragment of murine u-PA (mu-PA.1-48) to *u-PAR*$^{-/-}$ embryonic fibroblasts and macrophages.

***u-PAR*$^{-/-}$ mice displayed normal lysis of a murine plasma clot injected via the jugular vein. Invasion of macrophages into the peritoneal cavity after thioglycollate stimulation was similar in *u-PAR*$^{-/-}$ and *u-PAR*$^{+/+}$ mice. *u-PAR*$^{-/-}$ peritoneal macrophages had a threefold decreased initial rate of u-PA–mediated plasminogen activation in vitro but degraded extracellular matrix proteins in vitro as efficiently as *u-PAR*$^{+/+}$ macrophages.**

Thus, *u-PAR*$^{-/-}$ mice are viable, healthy, and fertile; they have a normal endogenous thrombolytic capacity but an impaired u-PA–mediated plasminogen activating potential. (*J. Clin. Invest.* 1996. 97:870–878.) Key words: gene targeting • embryonic stem cells • homologous recombination • extracellular proteolysis • fibrinolysis

Introduction

The identification on blood monocytes (1) and various other cell types (reviewed in reference 2) of a specific, high-affinity receptor for urokinase-type plasminogen activator (u-PA),[1] called the u-PA receptor (u-PAR), has suggested a role for the u-PA/u-PAR system in providing localized extracellular proteolytic activity. Its expression by a variety of migratory cells (reviewed in references 2–4) and more particularly its polarization at the leading edge of migrating cells (5, 6) has suggested involvement in cell invasion through extracellular matrices. Localized extracellular proteolysis may play a role in physiological processes such as macrophage invasion, ovulation, angiogenesis, wound healing, and in pathological conditions including inflammation and cancer metastasis (2–4, 7). The u-PAR was shown to be a highly glycosylated 55–60-kD cell surface protein linked to the cell membrane by a glycosylphosphatidylinositol anchor (8, 9). The mature protein consists of three homologous cysteine-rich domains, the first of which comprises the u-PA binding domain (10). The receptor binds both single-chain and two-chain u-PA without inactivation, thus concentrating plasmin generation at the cell surface (2); it may be involved in internalization of u-PA/inhibitor complexes (5, 11, 12) and in signal transduction (13–15).

The involvement of the u-PA/u-PAR system in the above described phenomena is largely deduced from indirect evidence. Additional evidence was obtained in mice deficient in u-PA, which show occasional fibrin depositions, enhanced endotoxin-induced thrombosis, impaired macrophage function, and greatly reduced neointima formation after arterial injury (16, 17). To establish the in vivo role of soluble versus receptor-bound u-PA, we have generated mice deficient in u-PAR and have analyzed the effect of *u-PAR* gene inactivation on viability, development, and reproduction, and on extracellular proteolytic capacity.

Portions of this study have been published in abstract form (1994, *Fibrinolysis.* 8 [Suppl. 1]: 51).

Preliminary data on the phenotype of u-PAR–deficient mice were reported by J. Degen et al. at the XIIth International Congress on Fibrinolysis and Thrombolysis, 18–22 September 1994 in Leuven, Belgium. Qualitatively, the results looked similar to those reported in the present study. These data were published during the revision of the present paper (Bugge, T.H., T.T. Suh, M.J. Flick, C.C. Daugherty, J. Romer, H. Solberg, V. Ellis, K. Danø, and J.L. Degen. 1995. The receptor for urokinase-type plasminogen activator is not essential for mouse development or fertility. *J. Biol. Chem.* 270:16886–16894.).

Address correspondence to R.C. Mulligan, Whitehead Institute for Biomedical Research, Nine Cambridge Center, Cambridge, MA 02142-1479. Phone: 617-258-5161; FAX: 617-258-5213. D. Collen, Center for Transgene Technology and Gene Therapy, VIB, Campus Gasthuisberg, O&N, Herestraat 49, B-3000 Leuven, Belgium. Phone: 32-16-345775; FAX: 32-16-345990; E-mail: Desire.Collen@med.kuleuven.ac.be

Received for publication 15 February 1995 and accepted in revised form 2 November 1995.

J. Clin. Invest.

0021-9738/96/02/0870/09 $2.00
Volume 97, Number 3, February 1996, 870–878

1. *Abbreviations used in this paper:* CNBr, cyanogen bromide; ES, embryonic stem; mABS, milliabsorbance; mu-PAR, murine u-PA receptor; PA, plasminogen activator; PGK, phosphoglycerokinase; PtdIns-PLC, phosphatidylinositol-specific phospholipase C; t-PA, tissue-type PA; u-PA, urokinase-type PA.

Methods

Animals. The mice were kept in microisolation cages on a 12 h day/night cycle and were fed regular chow. Housing and procedures involving experimental animals were performed in accordance with protocols approved by the Institutional Animal Care and Research Advisory Committee of the K. U. Leuven, Belgium.

Proteins and reagents. Human plasminogen, plasmin, fibrinogen, and cyanogen-bromide (CNBr)-digested fibrinogen were obtained and characterized as previously described (18). Recombinant human single-chain u-PA (hu-scu-PA) was kindly provided by Grünenthal AG, Aachen, Germany. Recombinant murine scu-PA (mu-scu-PA) was obtained using a recombinant baculovirus/insect cell expression system. The aminoterminal fragment of murine u-PA containing amino acid residues 1-48 (mu-PA.1-48) was kindly provided by Chiron Corporation, Emeryville, CA. Polyclonal rabbit anti–murine u-PAR antibody was a kind gift of F. Blasi (A.S. Raffaele Scientific Insititute, Milan, Italy). Phosphatidylinositol-specific phospholipase C (Ptd-Ins-PLC) from *Bacillus cereus* was obtained from Boehringer Mannheim (Brussels, Belgium).

Construction of the gene targeting vector. The *u-PAR* gene was isolated from a D_3 embryonic stem (ES) cell genomic DNA library (obtained from R. Jaenisch, Whitehead Institute, Massachusetts Intstitute of Technology, Cambridge, MA). A total homology of 8.3 kb was included into the parental *pPNT* vector which contains a *neomycin phosphotransferase* and a *Herpes simplex virus thymidine kinase* expression cassette (19), as outlined in Fig. 1. The gene encoding murine u-PAR is organized into 7 exons, of which exon 1 encodes the signal peptide; the three homologous domains are each encoded by two separate exons (20). In a first step, a 2.5-kb XhoI-ScaI fragment containing exons 6 and 7 was prepared in which the XhoI site was blunted and XbaI linkered. This fragment was then ligated into BamHI (blunted)-XbaI-restricted *pPNT*, yielding *pPNT.3′ u-PAR* (not shown). This ligation resulted in the deletion of the XhoI site and the generation of a novel XbaI site at the 5′ end of the 3′ flanking region (Fig. 1). Subsequently, a 5.8-kb BstEII fragment comprising exon 1 and ~ 4 kb upstream sequence was blunted, XhoI-linkered, and cloned into XhoI-restricted *pPNT.3′ u-PAR*. Correct orientation of the 5′ flanking region was verified by appropriate restriction digest analysis. The *neomycin resistance* gene expression cassette in the resultant targeting vector *pPNT.u-PAR* (Fig. 1) thus replaced a 10-kb genomic fragment comprising exons 2 through 5. This represents a deletion of the sequences encoding the aminoterminal two-thirds of the mature receptor protein which includes the u-PA binding domain (encoded by exons 2 and 3) as well as the region of alternative splicing (exon 4:5) (20, 21).

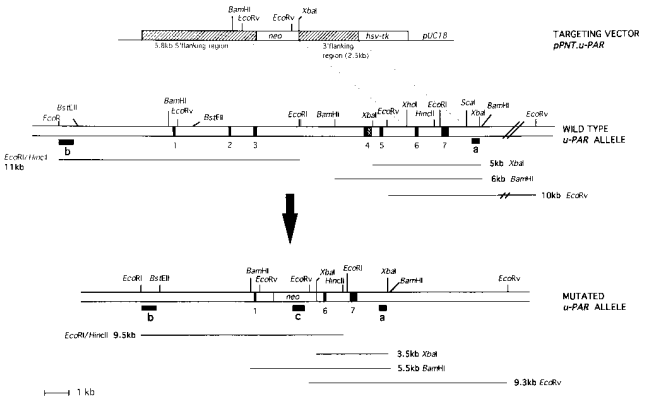

Figure 1. Outline of the strategy to disrupt the murine *u-PAR* gene. The targeting vector *pPNT.u-PAR* used for the inactivation of the *u-PAR* gene, the wild-type *u-PAR* allele, and the homologously recombined allele are schematically represented. The targeting vector contains the *neomycin resistance* gene (*neo*) and the *Herpes simplex virus thymidine kinase* gene (*hsv-tk*) to allow for double selection of homologous recombination events. Expression of *neo* and *hsv-tk* was under the control of the phosphoglycerokinase promoter (19). Transcription of both selectable marker genes was in the same direction as the endogenous *u-PAR* gene. Hatched areas represent the genomic fragments used as flanking regions in *pPNT.u-PAR.* Black boxes in the genomic structure represent exons. The cross-hatched area in exon 4 represents the sequence included in the alternatively spliced mu-PAR2 mRNA (21). Upon homologous recombination, the *neo* gene replaced a 10-kb genomic sequence comprising exons 2 through 5. The expected restriction fragments of the wild-type and the mutated allele are indicated with their relative size by underlining. Black boxes under the genes represent the probes used for Southern blot analysis. Probe *a* is a 0.2-kb StuI-XbaI genomic fragment located downstream of the 3′ flanking region. Probe *b* is a 0.8-kb EcoRI-BstEII genomic fragment located upstream of the 5′ flanking region. Probe *c* is a 0.6-kb Pst I fragment from the *neo* gene.

Generation of chimeric and u-PAR deficient mice. Targeted clones containing a disrupted *u-PAR* gene were injected into C57BL/6 (Harlan, LPB, The Netherlands) host blastocysts as described (24). Injected embryos were transferred into pseudopregnant $B6D_2F_1$ (Harlan) foster mothers. Chimeric animals, identified by the presence of agouti coat pigmentation, were test bred to C57BL/6 mice for germline transmission. Heterozygous u-PAR–deficient agouti offspring were identified by Southern blot analysis of tail tip genomic DNA. Brother-sister mating was carried out to generate homozygous u-PAR-deficient progeny.

Southern blot analysis of genomic DNA. DNA was isolated from ES cell clones or from mouse tail tips and was digested with the indicated restriction enzymes for Southern blot analysis as described (23, 25). Correct homologous recombination at the 3′ end was confirmed by hybridization of XbaI-, EcoRV- or BamHI-digested genomic DNA with a 0.2-kb StuI-XbaI fragment located downstream of the 3′ flanking region (Fig. 1, probe *a*). This probe detected a 5-kb XbaI wild-type and a 3.5-kb XbaI mutant fragment, a 6-kb BamHI wild-type and 5.5-kb BamHI mutant fragment, and a 10-kb EcoRV wild-type and 9.3-kb EcoRV mutant fragment (Fig. 1). To screen for correct homologous recombination at the 5′ end, a 0.8-kb EcoRI-BstEII fragment located upstream of the 5′ flanking region was used (Fig. 1, probe *b*) that detected an 11-kb EcoRI-HincII wild-type fragment and a 9.5-kb EcoRI-HincII mutant fragment (Fig. 1). To exclude additional random integration of the targeting vector, a 0.6-kb PstI fragment of the *neo* gene (Fig. 1, probe *c*) was used to verify the presence of a single 9.5-kb EcoRI-HincII fragment of the mutated allele.

Reverse transcriptase (RT)-PCR analysis. Primary embryonic fibroblast cells were prepared from 13.5-d-old *u-PAR*$^{+/+}$ or *u-PAR*$^{-/-}$ embryos using standard isolation and culture procedures (26). Polyadenylated RNA (polyA RNA) was extracted from the cells after a 24 h culture in the presence of 160 nM PMA, using the Quick Prep mRNA purification kit from Pharmacia Biotech Benelux (Roosendaal, The Netherlands) and was submitted to first-strand cDNA synthesis by oligo(dT) priming using the Pharmacia Ready-to-Go T-primed First Strand kit. The reaction products (RT-cDNA) were then used in PCR amplification with different sets of primers as indicated. PCR primers annealing in the *neo* gene were: 5′-ATTGAACAAGATGGATTGCAC-3′ (nt 744 to 764 in PMC1Neo; Stratagene, La Jolla, CA) (see Fig. 3, primer *a*) and 5′-TTCGTCCAGATCATCCTGATCGAC-3′ (nt 1220 to 1197 in PMC1Neo) (Fig. 3, reverse primer *b*). PCR primers annealing in *mu-PAR*, with nucleotide numbering according to the mu-PAR1.cDNA sequence (21), were : 5′-CAACAGGACCATGAGTTACCGCATGG-3′ (nt 233 to 258; Fig. 3 *B*, exon 3 primer), 5′-AGTGGGTGTAGTTGCAACACTTCAG-3′ (nt

600 to 576; Fig. 3 *B*, exon 5 reverse primer), 5′-TGCTGTTGCTGGCGACTACCTGTGTC-3′ (nt 40 to 65; Fig. 3, exon 1 primer *c*), 5′-TCAGGTCCAGAGGAGGACGCCCCATAGTCC-3′ (nt 995 to 966; Fig. 3, exon 7 reverse primer *d*), and 5′-TTGATGAGAGACGCCTCTTCGGAGGAAC-3′ (nt 705–688; Fig. 3, exon 6 reverse primer *e*). The RT-PCR products were analyzed by separation on a 1% agarose gel. PCR amplification products were purified directly using the QIAquick Spin PCR Purification Kit or from the agarose gel using the QIAquick Gel Extraction Kit (Qiagen, Westburg, Leusden, The Netherlands). The purified DNA was then subjected to cycle-sequencing using the Pharmacia Auto Cycle Sequencing kit with FITC-labeled primers annealing at different sites within mu-PAR exon 1 (sense primers), exon 6 or 7 (antisense primers), or in the *neo* gene (sense primers).

ELISA assay on coated embryonic fibroblast cells. Primary embryonic fibroblast cells prepared from *u-PAR*$^{+/+}$, *u-PAR*$^{+/-}$, or *u-PAR*$^{-/-}$ embryos were plated at a density of 60,000 cells/well on 96-well plates after gelatinization of the wells for 10 min with 0.2% gelatin. After overnight culture, the cells were incubated for 2 h with DME (Gibco BRL, Life Technologies, Merelbeke, Belgium) without or with phosphatidylinositol phospholipase C (final concentration of 2 U/ml) in the absence of serum. The wells were washed with PBS and blocked for 1 h at 37°C with gelatin (200 μl/well of a 3% solution in PBS). The cells were then incubated for 1 h at room temperature with purified rabbit anti–murine u-PAR (final concentration 30 μg/ml) or with an irrelevant polyclonal antibody (rabbit anti–murine IgG, final concentration 10 μg/ml) (Dako-Immunoglobulins, Prosan, Ghent, Belgium) and washed three times with PBS containing 0.1% BSA and 0.002% Tween 80. Bound rabbit anti–murine u-PAR was detected using horseradish peroxidase–labeled goat anti–rabbit IgG (Bio-Rad Laboratories, Richmond, CA) (1:2,000 dilution, 1 h incubation at room temperature) preincubated for 2 h at room temperature with preimmune mouse serum (10% final concentration). Binding was determined as the optical density at 405 nm measured 30 min after addition of peroxidase substrate. Values obtained in a series of control wells incubated with buffer instead of rabbit polyclonal antibodies were used to correct for background binding of the secondary antibody.

Isolation of in vivo–stimulated peritoneal macrophages. Peritoneal exudate cells were obtained from 4 to 6–wk-old *u-PAR*$^{+/+}$, *u-PAR*$^{+/-}$, and *u-PAR*$^{-/-}$ mice 3 d after intraperitoneal injection of 0.5 ml of a 4% solution of thioglycollate (Difco Laboratories Inc., Detroit, MI). To collect the cells, the peritoneal cavity was flushed with 5 ml of a sterile 5% glucose solution. Total cell count was determined using a Coulter Counter, model DN (Coulter Electronics Ltd, Dunstable, England). Cells were washed with regular culture medium consisting of DME containing 4.5 g/liter glucose (Gibco BRL), 10% FBS (Hyclone, Greiner, Wemmel, Belgium), 100 U/ml penicillin, 0.1 mg/ml streptomycin, and 2 mM glutamine (Gibco BRL). The cells were resuspended in the appropriate medium and counted again before use.

Ligand binding assay. Peritoneal exudate cells from thioglycollate-treated mice were plated in 96-well microtiter plates at a density of 200,000 cells per well and incubated overnight in regular culture medium. The cultures were washed twice with DME to remove nonadherent cells. These purified macrophage cultures were then washed with 50 mM glycine-HCl buffer, pH 3.0, containing 100 mM NaCl for 3 min to dissociate surface-bound endogenous u-PA, and neutralized with a 0.2 vol of 500 mM Hepes buffer, pH 7.5, containing 100 mM NaCl. The plates were washed once with DME containing 0.1% BSA (binding medium) and 100 μl binding medium containing 2 nM ^{125}I-labeled mu-PA.1-48 without or with increasing concentrations of competitor (unlabeled mu-PA.1-48, unlabeled murine scu-PA or human scu-PA) was added. After incubation for 1 h at room temperature, the cells were washed three times with binding medium (200 μl per well) and lysed with 100 μl 1N NaOH. The lysate of each well was transferred separately to an eppendorf tube and counted for bound radiolabel. Results were corrected for background using values obtained from similarly treated wells containing no cells (typically around 100 cpm).

^{125}I-fibrin–labeled plasma clot lysis in vivo. Lysis of a ^{125}I-fibrin–labeled murine plasma clot injected via a jugular vein and embolized into the pulmonary arteries was monitored, essentially as previously described (27). Briefly, a 25 μl ^{125}I-fibrin–labeled plasma clot containing ~ 70,000 cpm human ^{125}I-fibrin (0.07 μCi) was prepared from a plasma pool of wild-type mice and was injected into the jugular vein. Spontaneous clot lysis was evaluated by measuring the residual radioactivity in the heart and lungs at the indicated time points and was defined as the amount of radioactivity which had disappeared, expressed in percentage of the total amount of radioactivity injected.

Preparation and lysis of [^{3}H]proline–labeled subendothelial matrix by thioglycollate-stimulated peritoneal macrophages. [^{3}H]proline–labeled matrix from human umbilical vein endothelial cells was prepared in 24-well dishes as described (28). Peritoneal cells from thioglycollate-injected mice were plated on the [^{3}H]proline matrix at a density of 10^6 cells per well in medium A (DME containing 0.02% lactalbumin hydrolysate, 100 U/ml penicillin, 0.1 mg/ml streptomycin, 2 mM glutamine, and 10 U/ml aprotinin [Trasylol, Bayer, Leverkusen, Germany]) and incubated for 1 h at 37°C in a CO_2-incubator (5% CO_2, 90% humidity). Nonadherent cells as well as the protease inhibitor aprotinin present in medium A were then removed by washing twice with medium B (medium A without aprotinin). The cells were finally refed with 500 μl per well of medium B with or without 2 μg/ml human plasminogen, and the cells were returned to the incubator. At the time intervals indicated, 50 μl aliquots of the medium were removed after gentle mixing and were counted to determine released radiolabel. Control wells without cells were used for background correction, and control wells without cells were treated with excess trypsin for determination of total (100%) radioactivity incorporated.

Plasminogen activation by cell-associated endogenous u-PA. Peritoneal exudate cells from thioglycollate-injected mice were plated in 96-well microtiter plates at a density of 50,000 cells per well in medium A. After overnight incubation at 37°C in 5% CO_2 and 90% humidity, the plates were washed extensively with medium B. 200 μl aliquots of PBS containing 1 mg/ml BSA, 2.5 μM human plasminogen, and 0.3 mM S2403 (Chromogenix, Antwerp, Belgium) without or with CNBr-digested human fibrinogen (final concentration 0.25 μM) or amiloride hydrochloride (final concentration 300 μM) (Sigma Chemical Company, NTL, Brussels, Belgium) were added, and generated plasmin activity was quantified by recording the change in absorbance at 405 nm. Background absorbance was determined by incubating cells with S2403 in the absence of plasminogen. Activation of human plasminogen by murine u-PA or tissue-type plasminogen activator (t-PA) in the presence or absence of CNBr-fragments of human fibrinogen has been characterized elsewhere (29).

Histology. *u-PAR*$^{+/+}$, *u-PAR*$^{+/-}$, and *u-PAR*$^{-/-}$ mice, aged 4.5 wk, were killed with an overdose of Avertin (2,2,2-tribromoethanol; Aldrich Chemie, Bornem, Belgium) for tissue collection. The tissues were fixed in phosphate-buffered 4% formaldehyde, pH 7.0, and embedded in paraffin, and representative sections (5 μm, hematoxylin-eosin stained) of brain, leg muscle, lung, heart, kidney, liver, intestinal tissue, stomach, reproductive organs, thyroid, and thymus were selected for histopathological examination.

Statistical analysis. The statistical significance of differences between groups was determined using Student's *t* test or Chi-square analysis.

Results

Targeting of the u-PAR gene. Inactivation of the murine *u-PAR* gene was achieved using a replacement-type targeting vector in which a *neomycin phosphotransferase* gene replaced a 10-kb *u-PAR* genomic fragment comprising the exons encoding domain 1 (the u-PA binding domain) and domain 2 of the mature u-PAR protein (exons 2 through 5), including the region of alternative splicing (Fig. 1). Thus, correct targeting would effectively abolish *u-PAR* gene expression. The linearized targeting

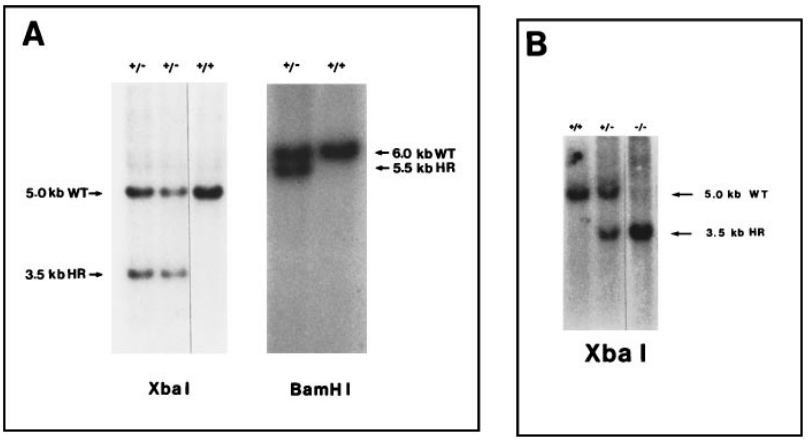

Figure 2. Southern blot analysis of genomic DNA. (*A*) Southern blot analysis of genomic DNA from D_3 embryonic stem cell clones, digested with XbaI or BamHI and hybridized to the 3′ flanking probe *a* (Fig. 1). The appearance of a novel 3.5-kb (XbaI digest) or 5.5-kb (BamHI digest) band indicates correct targeting. (*B*) Southern blot analysis of tail tip genomic DNA from *u-PAR*$^{+/+}$, *u-PAR*$^{+/-}$, and *u-PAR*$^{-/-}$ mice digested with XbaI and hybridized with the 3′ flanking probe *a* (Fig. 1). The 5.0- and 3.5-kb bands indicate the presence of the wild-type or mutated allele, respectively. *WT*, wild-type; *HR*, homologously recombined.

construct was electroporated in D_3 ES cells (genetic background 129 [22]) and Southern blot analysis of genomic DNA identified 19 targeted clones out of 728 G418^r-Ganc^r colonies analyzed, representing an overall frequency of homologous recombination of 1:40. Correctly targeted clones displayed the expected fragments after Southern blot analysis using probe *a* (Fig. 1) with XbaI- or BamHI-restricted genomic DNA (Fig. 2 *A*). Likewise, Southern blotting of EcoRV-restricted genomic DNA with probe *a* and of EcoRI-HincII restricted genomic DNA with probe *b* or probe *c* (Fig. 1) displayed the expected fragments (data not shown). The *neo*-specific probe *c* was used to verify single integration of the targeting construct at the *u-PAR* locus by exclusive generation of a 9.5-kb EcoRI-HincII mutant fragment. Southern blot analysis results were confirmed after expansion of the individual targeted clones (not shown).

Germline transmission of the inactivated u-PAR allele. Four independent homologous recombinants were injected into C57BL/6 host blastocysts. With one of these, 11 chimeric mice were obtained (1 female and 1 male with 30–40% chimerism, 4 males with 60–85% chimerism and 5 males with ≥ 90% chimerism). Upon mating to C57BL/6 mice, all chimeras except the female (30% chimerism) and one male (95% chimerism) transmitted the ES cell DNA through the germline as indicated by the presence of agouti pups among their offspring.

Viability, fertility, and growth of u-PAR–deficient mice. Agouti offspring (F_1 generation) obtained from the matings of the chimeric males with C57BL/6 females were genotyped by Southern blot analysis of tail tip DNA (not shown). The heterozygous (*u-PAR*$^{+/-}$) mice were intercrossed and their F_2 offspring was genotyped. Fig. 2 *B* shows a Southern blot analysis using probe *a* with XbaI-digested tail tip genomic DNA from *u-PAR*$^{+/+}$, *u-PAR*$^{+/-}$, and *u-PAR*$^{-/-}$ littermates. Among 274 F_2 littermates analyzed, 57 were *u-PAR*$^{+/+}$ (21%), 147 were *u-PAR*$^{+/-}$ (54%), and 70 were *u-PAR*$^{-/-}$ (25%). This distribution is not significantly different (Chi-square test) from the expected mendelian 1:2:1 ratio, indicating equal viability of *u-PAR*$^{+/+}$, *u-PAR*$^{+/-}$, and *u-PAR*$^{-/-}$ mice.

u-PAR deficiency did not affect the growth of young animals: at 4.5 wk of age, body weight values (mean±SEM) were 20±0.8 g (n = 6) for *u-PAR*$^{-/-}$ males versus 24±0.5 g (n = 4) for *u-PAR*$^{+/+}$ males (P = 0.36), and 16±1.2 g (n = 5) for *u-PAR*$^{-/-}$ females versus 17±0.7 g (n = 3) for *u-PAR*$^{+/+}$ females (P = 0.57). u-PAR deficiency did not appear to affect fertility as evidenced by similar sizes and numbers of litters produced by *u-PAR*$^{-/-}$ as compared to *u-PAR*$^{+/+}$ breeding pairs.

RT-PCR analysis. *u-PAR*$^{+/+}$ and *u-PAR*$^{-/-}$ mice were analyzed at the RNA level by RT-PCR using polyA RNA extracted from PMA-stimulated primary embryonic fibroblast cells (Fig. 3). PCR with an upstream primer annealing in exon 3 and a downstream primer annealing in exon 5 (Fig. 3 *B*) confirmed the absence of *u-PAR* exon 3 through exon 5 sequences in *u-PAR*$^{-/-}$ derived messages (Fig. 3 *B*, lane *6*). PCR reactions performed with a set of primers annealing within the *neo* gene (Fig. 3 *A*, primers *a*, *b*) confirmed the presence of the *neo* gene in genomic DNA isolated from tail tissue of a *u-PAR*$^{-/-}$ mouse (Fig. 3 *C*, lane *4*) and showed expression of the gene in *u-PAR*$^{-/-}$ fibroblasts (Fig. 3 *C*, lane *6*).

PCR with a primer set annealing in exon 1 and exon 7 (Fig. 3 *A*, primers *c*, *d*) yielded a single PCR product of the expected size (950 bp) for wild-type cDNA (Fig. 3 *D*, lane *5*). PCR on *u-PAR*$^{-/-}$ RT-cDNA with this primer set generated two bands of ~ 400 and 260 bp, respectively (Fig. 3 *D*, lane *6*). The size of the 400-bp band corresponded to the size expected for exon 1/exon 6/exon 7 splicing. The size of the 260 bp product suggested splicing from exon 1 to exon 7. Cycle-sequencing (not shown) of these PCR products after purification from the agarose gel, confirmed this to be indeed the case. Splice junctions showed the expected sequences which retain the *u-PAR* reading frame. Consequently, domain fragments of the receptor could be expressed from the inactivated alleles. However, as shown below in binding and competition experiments, no evidence was found for the presence of u-PA binding activity on *u-PAR*$^{-/-}$ cells. An intensity difference between the 400-bp and 260-bp RT-PCR products was observed (Fig. 3 *D*, lane *6*), suggesting a higher abundance of the exon 1/exon 7 splice variant. The relative intensities of the two bands were determined by densitometry of computer images of agarose gels (Stratagene EagleEye-II Still Video System; Stratagene, Westburg, Leusden, The Netherlands), using the NIH Image 1.59b5 program, yielding a relative intensity of 81±7% for the 260 bp product (mean±SD obtained from measurements on nine independent PCR reactions).

To verify run-through transcription from the phosphoglycerokinase (PGK) promoter driving the expression of *neo*, PCR reactions were performed using a forward primer annealing in the *neo* gene and a reverse primer annealing in exon 6 (Fig. 3 *A*, primers *a*, *e*). As expected, genomic DNA from *u-PAR*$^{-/-}$ mice yielded a 1.74-kb product (Fig. 3 *E*, lane *4*) while no am-

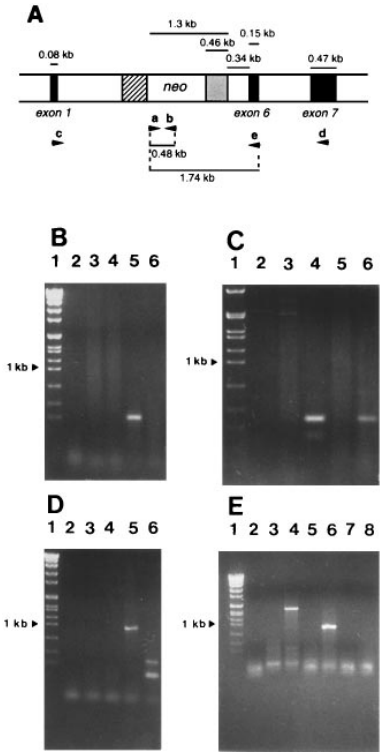

Figure 3. RT-PCR analysis of polyA RNA isolated from PMA-stimulated *u-PAR*$^{+/+}$ and *u-PAR*$^{-/-}$ embryonic fibroblast cells. (*A*) Schematic representation of the targeted allele (see also Fig. 1). Sizes of gene fragments are indicated above the construct. The arrowheads *a–e* represent the PCR primers used in panels *C–E* of this figure. The size of potential PCR products is indicated below the construct. Hatched and dotted regions in the construct represent the PGK promoter and polyA signal, respectively. (*B*) PCR products generated using an upstream and downstream primer annealing in exon 3 and exon 5, respectively. An amplification product of about 370 bp is expected with this primer set for wild-type cDNA. (*C–E*) PCR products generated using primer set *a*:*b* (*C*), primer set *c*:*d* (*D*), or primer set *a*:*e* (*E*), and separated by electrophoresis on a 1% agarose gel. Lane 1: DNA molecular weight markers of 8, 7.1, 6, 4.8, 3.5, 2.7, 1.9, 1.85, 1.5, 1.4, 1.15, 1.0, 0.68, 0.49, and 0.37 kb; lane *2*: PCR reaction without DNA template; lane *3*: PCR with genomic DNA from tail tissue of a *u-PAR*$^{+/+}$ mouse; lane *4*: PCR with genomic DNA from tail tissue of a *u-PAR*$^{-/-}$ mouse; lane *5*: PCR on a first strand cDNA template generated from polyA RNA isolated from *u-PAR*$^{+/+}$ embryonic fibroblast cells; lane *6*: PCR on a first strand cDNA template generated from polyA RNA isolated from *u-PAR*$^{-/-}$ embryonic fibroblast cells; lane *7*: PCR on polyA RNA isolated from *u-PAR*$^{+/+}$ cells; lane *8*: PCR on polyA RNA isolated from *u-PAR*$^{-/-}$ cells. The polyA RNA preparations were free of genomic DNA as indicated by the absence of amplification products when using polyA RNA as template (see *E*, lane *8* for *u-PAR*$^{-/-}$ preparations; not shown for wild-type).

plification product was obtained with genomic DNA from *u-PAR*$^{+/+}$ mice (Fig. 3 *E*, lane *3*). Likewise, RT-cDNA generated from *u-PAR*$^{+/+}$ mRNA did not yield any amplification product (Fig. 3 *E*, lane *5*). RT-cDNA template from *u-PAR*$^{-/-}$ mRNA however yielded a PCR product of $\sim$ 0.9 kb (Fig. 3 *E*, lane *6*). This 0.9-kb product likewise was subjected to cycle sequencing (not shown). The sequencing results indicated cryptic splicing of a full-length *neo* message including its STOP codon and part of the PGK polyadenylation site of the *neo* cassette, to exon 6 of *u-PAR*. The presence of the *neo* STOP codon however ensures termination of translation at this site, excluding the expression of a neo/u-PAR–domain 3 fusion protein. The presence of several STOP codons in both other reading frames of the *neo* gene similarly excludes the expression of domain 3 from run-through messages driven by the PGK promoter of the *neo* cassette but starting erroneously at an out-of-frame ATG codon in the *neo* sequence.

ELISA for murine u-PAR. The presence or absence of mu-PAR protein on the cell surface was verified in an ELISA assay on cultures of primary embryonic fibroblast cells using a polyclonal anti-murine u-PAR antibody (Fig. 4). Binding (expressed in milliabsorbance (mABS) at 405 nm) of the antibody to *u-PAR*$^{+/+}$ or *u-PAR*$^{+/-}$ fibroblasts was respectively 1.90- and 1.36-fold higher (Fig. 4) than binding to *u-PAR*$^{-/-}$ cells (140$\pm$4.4 for *u-PAR*$^{+/+}$ and 100$\pm$0.5 for *u-PAR*$^{+/-}$ cells versus 74$\pm$4.6 for *u-PAR*$^{-/-}$ cells, mean$\pm$SEM, $n = 3$, $P \leq 0.005$, not shown). Such a difference was not observed with an irrelevant polyclonal rabbit anti–mouse antibody (Fig. 4). Binding of rabbit anti–murine u-PAR to *u-PAR*$^{+/+}$ or *u-PAR*$^{+/-}$ cells decreased to the level obtained with *u-PAR*$^{-/-}$ cells after cleavage of the receptor upon treatment with Ptd-Ins-PLC (77$\pm$4.8 mABS for *u-PAR*$^{+/+}$ and 77$\pm$9.8 mABS for *u-PAR*$^{+/-}$ cells versus 74$\pm$4.6 mABS for untreated *u-PAR*$^{-/-}$ cells, mean$\pm$SEM, $n = 3$, $P > 0.6$, not shown) (Fig. 4). Values obtained for *u-PAR*$^{-/-}$ cells without or with Ptd-Ins-PLC treatment were similar (66$\pm$4.6 mABS with versus 74$\pm$4.6 mABS without treatment, mean$\pm$SEM, $n = 3$, $P = 0.286$, not shown) (Fig. 4). Treatment of the cells with Ptd-Ins-PLC did not significantly affect the interaction with the irrelevant antibody (P values $>$ 0.5) (Fig. 4). These results indicated that the level of binding of the anti–murine u-PAR antibody to *u-PAR*$^{-/-}$ cells or to Ptd-Ins-PLC treated *u-PAR*$^{+/+}$ or *u-PAR*$^{+/-}$ cells represented aspecific binding and that interaction of untreated cells with the antibody was gene dose dependent. Comparable cell counts for *u-PAR*$^{+/+}$, *u-PAR*$^{+/-}$, and *u-PAR*$^{-/-}$, as determined in a series of control wells processed through the assay using buffer in all steps, excluded any effect of differences in cell number at the end of the experiment.

Ligand binding assay. A binding assay was performed on peritoneal macrophages isolated from *u-PAR*$^{+/+}$, *u-PAR*$^{+/-}$, or *u-PAR*$^{-/-}$ mice using an aminoterminal fragment of murine u-PA (mu-PA.1-48) as the ligand (Fig. 5). This fragment contains the growth factor domain of urokinase which constitutes the receptor binding part of the molecule (30).

Binding of ^{125}I-mu-PA.1-48 to *u-PAR*$^{+/+}$ macrophages reached a value of 2,000$\pm$300 cpm and was decreased to 220$\pm$50, 48$\pm$16, and 34$\pm$23 cpm in the presence of unlabeled mu-PA.1-48, or to 56$\pm$15, 100$\pm$19, and 36$\pm$23 cpm in the pres-

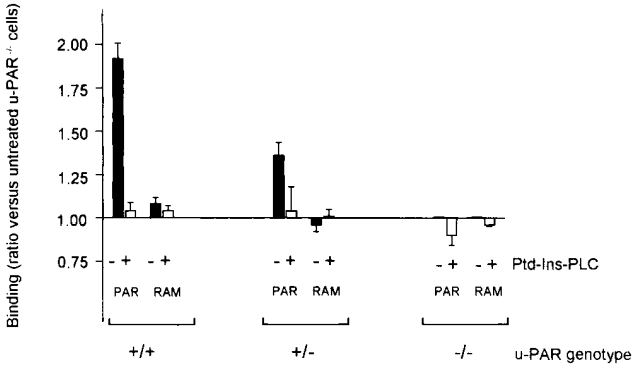

Figure 4. ELISA assay for murine u-PAR. Binding of polyclonal rabbit anti–murine u-PAR (*PAR*) or of the irrelevant antibody rabbit anti–mouse IgG (*RAM*) to primary embryonic fibroblast cells without (*filled bars*) or with (*open bars*) pretreatment of the cells with phosphatidylinositol specific phospholipase C (*Ptd-Ins-PLC*) was determined as described in Methods. Binding was measured as optical density at 405 nm and is expressed as the ratio versus untreated *u-PAR*$^{-/-}$ cells. Data represent mean values$\pm$SEM obtained from three independent experiments performed in triplicate.

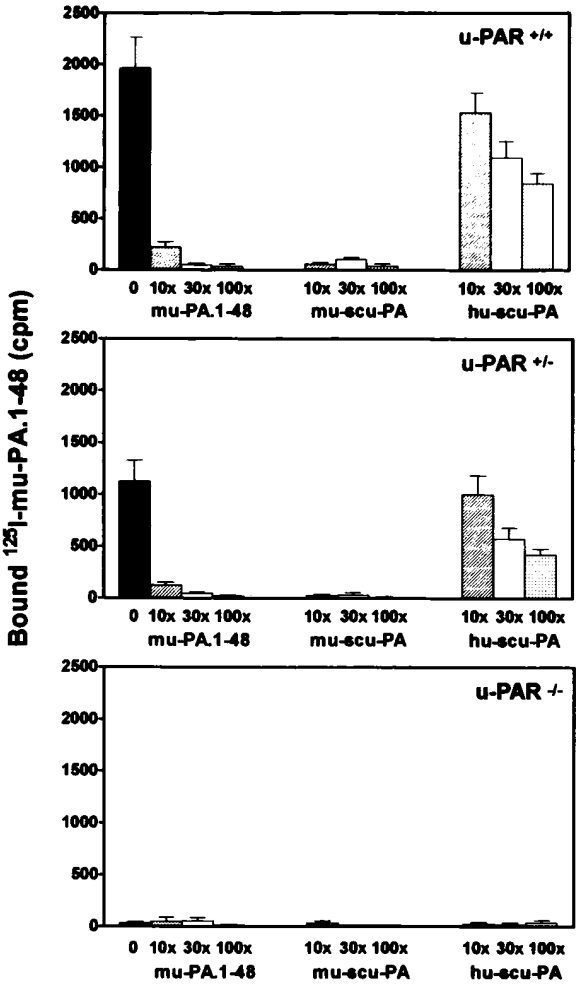

Figure 5. Binding of murine u-PA aminoterminal fragment mu-PA.1-48 to thioglycollate stimulated peritoneal macrophages from *u-PAR*$^{+/+}$ (*top*), *u-PAR*$^{+/-}$ (*middle*), and *u-PAR*$^{-/-}$ (*bottom*) mice. Purified macrophage cultures were prepared in microtiter plates by overnight incubation of peritoneal lavages and removal of nonadherent cells by vigorous washing. After acid treatment to dissociate surface bound murine u-PA, the cultures were incubated for 1 h with 2 nM ^{125}I-labeled mu-PA.1-48 without or with unlabeled competitor (mu-PA.1-48, murine scu-PA or human scu-PA) at 10- to 100-fold molar excesses as indicated. The cells were washed three times, lysed with 1 N NaOH, and removed from the plate for γ-counting. Data represent mean values with SEM obtained from four to seven independent experiments.

ence of unlabeled intact murine scu-PA at a 10-, 30-, or 100-fold molar excess, respectively (mean±SEM, $n = 5$) (Fig. 5, *top*), demonstrating the specificity of the binding. A much less dramatic decrease in binding was obtained in the presence of human scu-PA (1,500±190, 1,100±160, and 840±100 cpm bound at a 10-, 30-, or 100-fold molar excess, respectively, versus 2,000±300 cpm without competition, $n = 5$; $P < 0.05$ for the data obtained at 30- and 100-fold molar excess), in agreement with the reported species specificity of the u-PA/u-PAR interaction (31). This species specificity was however not absolute, as shown by the moderate inhibition obtained, presumably due to the partial homologies between murine and human u-PA and u-PAR.

Binding of ^{125}I-mu-PA.1-48 to *u-PAR*$^{+/-}$ macrophages was about half of that obtained with wild-type cells (1,100±210 cpm bound, mean±SEM, $n = 7$, versus 2,000±300 cpm for wild-type cells, $n = 5$, $P < 0.05$) and was also significantly inhibited in the presence of unlabeled mu-PA.1-48 (120±30, 44±14, and 19±9 cpm bound at a 10-, 30-, or 100-fold molar excess) or of intact murine scu-PA (23±13, 29±22, and 10±5 cpm at a 10-, 30-, or 100-fold molar excess) (Fig. 5, *middle*). Much less pronounced inhibition was observed in the presence of human scu-PA (1,000±180, 570±110, and 420±57 cpm bound at a 10-, 30-, or 100-fold molar excess, respectively, versus 1,100±210 cpm without competition, $n = 7$; $P < 0.05$ for the data obtained at a 30- and 100-fold molar excess).

Binding of ^{125}I-mu-PA.1-48 to *u-PAR*$^{-/-}$ macrophages was 33±12 cpm (mean±SEM, $n = 4$) and was not statistically different from the binding obtained in the presence of unlabeled mu-PA.1-48 (50±38, 55±29, and 4±2 cpm at a 10-, 30-, or 100-fold molar excess, $n = 4$, P values versus binding without competition > 0.05) or of intact murine scu-PA (34±18 cpm at 10-fold molar excess, P value versus no competition 0.97; binding at higher molar excess < 4 cpm) (Fig. 5, *bottom*). The binding obtained in the absence of competitor with *u-PAR*$^{-/-}$ cells was 1.7% of that obtained with *u-PAR*$^{+/+}$ cells (33±12 cpm, $n = 4$, versus 2,000±300 cpm for wild-type cells, $n = 5$; $P < 0.001$) and was comparable to the background binding to *u-PAR*$^{+/+}$ or *u-PAR*$^{+/-}$ cells as measured in the presence of a 100-fold molar excess of mu-PA.1-48 (33±12 cpm for *u-PAR*$^{-/-}$ cells, $n = 4$, versus 34±23 cpm for *u-PAR*$^{+/+}$ cells, $n = 5$, $P = 0.97$, and versus 19±9 cpm for *u-PAR*$^{+/-}$ cells, $n = 7$, $P = 0.37$). These results indicated that the binding obtained with *u-PAR*$^{-/-}$ cells only represented aspecific binding.

Similar results were obtained in ^{125}I-mu-PA.1-48 binding experiments using embryonic fibroblast cells isolated from *u-PAR*$^{+/+}$ or *u-PAR*$^{-/-}$ embryos (not shown).

^{125}I-fibrin–labeled plasma clot lysis in vivo. Spontaneous in vivo lysis of a ^{125}I-fibrin–labeled murine plasma clot, injected into the jugular vein and embolized to the lungs, was similar in *u-PAR*$^{+/+}$ (groups of three or two mice in the 4 and 24 h time group, respectively) and *u-PAR*$^{-/-}$ mice (groups of three mice). Mean±SEM values at 4 h were 49±10% and 61±5%, respectively, and at 24 h 93±3% and 98±0.4%, respectively. These data are in accordance with the in vivo plasma clot lysis results obtained previously in u-PA–deficient mice, and with the notion that, in contrast to t-PA, u-PA plays only a minor role in in vivo thrombolysis (16).

Macrophage function. Invasion of macrophages into the peritoneal cavity measured 3 d after intraperitoneal injection of thioglycollate was not affected by *u-PAR* gene inactivation: cell counts in peritoneal lavages were 9.2±1.4, 10±1.2, and 9.5±1.5 × 10^6 cells (mean±SEM, $n = 7$, $P > 0.8$) for *u-PAR*$^{+/+}$, *u-PAR*$^{+/-}$, and *u-PAR*$^{-/-}$ mice, respectively, assuming that 80–90% of the cells are macrophages (32). Thioglycollate stimulated macrophages from u-PA–deficient mice have a reduced capacity to degrade subendothelial matrix (16). To examine whether this u-PA–mediated breakdown in vitro was u-PAR dependent, lysis of subendothelial matrix metabolically labeled with [^{3}H]proline was studied using stimulated macrophages from *u-PAR*$^{+/+}$, *u-PAR*$^{+/-}$, and *u-PAR*$^{-/-}$ mice. No differences in matrix degradation were found between the different genotypes (P values > 0.25). Approximately 30% of the activity measured in this matrix degradation assay was however plasminogen-independent (Fig. 6).

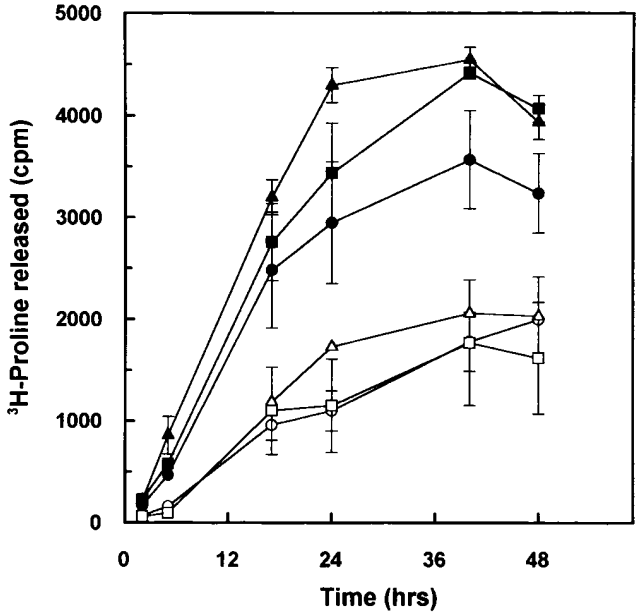

Figure 6. Lysis of [^{3}H]proline–labeled subendothelial matrix by thioglycollate-stimulated macrophages from *u-PAR*$^{+/+}$ (●, ○), *u-PAR*$^{+/-}$ (■, □) or *u-PAR*$^{-/-}$ (▲, △) mice. The experiment was performed without (*open symbols*) or with (*closed symbols*) 2 μg/ml human plasminogen in the culture medium. The data represent mean values with SEM obtained from two to five independent experiments.

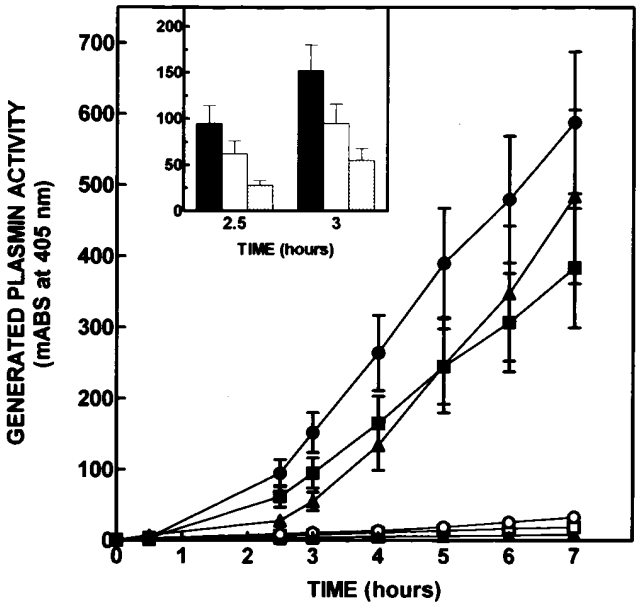

Figure 7. Plasmin activity generated upon incubation of in vivo–stimulated macrophages in the presence of plasminogen and of the chromogenic plasmin substrate S2403. Macrophages were harvested from the peritoneal cavity 3 d after intraperitoneal injection of thioglycollate in *u-PAR*$^{+/+}$ (●, ○), *u-PAR*$^{+/-}$ (■, □) or *u-PAR*$^{-/-}$ (▲, △) mice. The experiment was performed in the absence (*closed symbols*) or presence (*open symbols*) of 300 μM of the u-PA inhibitor amiloride. *Insert*: Bar graph representation of the data obtained at 2.5 and 3 h in the absence of amiloride with *u-PAR*$^{+/+}$ (*filled bars*), *u-PAR*$^{+/-}$ (*open bars*), and *u-PAR*$^{-/-}$ macrophages (*hatched bars*). Data represent mean values with SEM obtained from duplicate measurements in three independent experiments.

Plasminogen activation in vitro by thioglycollate-stimulated macrophages in the presence of human plasminogen and of the chromogenic plasmin substrate S2403 was virtually completely inhibited by amiloride (Fig. 7) but was not affected by CNBr-fragments of fibrinogen (not shown) indicating that the plasmin generation was u-PA–mediated. Within 2.5–3 h, plasminogen activation was twofold lower with *u-PAR*$^{-/-}$ than with *u-PAR*$^{+/-}$ macrophages (OD at 405 nm of 28±5 and 55±13 mABS for *u-PAR*$^{-/-}$ cells at 2.5 and 3 h, respectively, versus 62±14 and 95±36 mABS for *u-PAR*$^{+/-}$ cells, mean± SEM, $n = 3$, $P > 0.05$) and threefold lower than with *u-PAR*$^{+/+}$ macrophages (28±5 and 55±13 mABS versus 95±19 and 150±30 mABS for *u-PAR*$^{+/+}$ macrophages at 2.5 and 3 h, respectively, $n = 3$, $P < 0.05$) (Fig. 7, *inset*). Freshly washed cells were used to ensure that at the initial time points only endogenous, receptor-bound u-PA was mediating the plasmin generation. At later time points, the statistically significant difference between *u-PAR*$^{-/-}$ and *u-PAR*$^{+/+}$ macrophages disappeared (Fig. 7), presumably due to increasing contribution of murine u-PA accumulating in the medium.

Histological examination. No significant histological abnormalities could be documented on microscopic examination of tissues from 4.5-wk-old *u-PAR*$^{-/-}$ mice.

Discussion

To study the role of receptor-binding in the physiological functions of u-PA, mice with inactivated *u-PAR* genes were generated via homologous recombination in embryonic stem cells. Inactivation was achieved by replacing a genomic fragment comprising exon 2 through 5 by a *neo* selection marker cassette. Southern blot analysis of genomic DNA isolated from tail tissue confirmed the presence of the targeted alleles in the *u-PAR*$^{+/-}$ and *u-PAR*$^{-/-}$ mice.

Inactivation of the *u-PAR* gene yielded a mutated allele containing the u-PAR promoter and the exon 1, 6 and 7 sequences, disrupted between exon 1 and 6 by the *neo* cassette. Exon 6 and 7 together encode domain 3 of the receptor (20). To verify whether aberrant messages were expressed from the inactivated allele, potentially generating a truncated "domain 3" receptor, RT-PCR analysis was performed on polyA RNA isolated from PMA-stimulated embryonic fibroblast cells. RT-PCR analysis indeed revealed the presence of truncated u-PAR messages in the *u-PAR*$^{-/-}$ mice. Cycle-sequencing was performed to identify the nature of the three different kinds of messages obtained. Two messages, identified by PCR amplification of *u-PAR*$^{-/-}$ RT-cDNA with a single PCR primer set, were expressed from the u-PAR promoter and consisted of an exon 1/exon 6/exon 7 and an exon 1/exon 7 splice product, respectively. The u-PAR reading frame was retained in both messages. Consequently, a domain 3 receptor might theoretically be expressed from the largest message. However, as discussed below, no evidence for the presence of u-PA binding activity on *u-PAR*$^{-/-}$ cells was found. In addition, the exon 1/exon 7 splice variant appeared to be present at higher abundance as compared to the exon 1/exon 6/exon 7 variant (81% versus 19%). If translated, the former message would only generate the second half of domain 3 of u-PAR. Such a half domain very unlikely would retain functions of intact u-PAR. Moreover, the odd number of cysteines in the second half of

domain 3 of murine u-PAR (21) might cause folding and stability problems. Furthermore, exon 1 only encodes the first 19 amino acid residues of the u-PAR signal peptide. The last amino acids, and thus also the processing cleavage site, are encoded by exon 2 which is absent from the inactivated alleles. Computer-aided amino acid sequence analysis of both splice variants did not reveal the presence of new signal peptide processing sites. This truncation of the signal peptide and absence of a consensus processing site probably would interfere with proper secretion and processing of potentially translated u-PAR protein fragments. Furthermore, if expression would indeed occur, these fragments would be expected to be nonfunctional. Previous studies indeed have shown that domain fragments of u-PAR are incapable of ligand binding (3, 33). A third message, consisting of a *neo/exon 6* fusion message expressed from the PGK promoter of the *neo* cassette, arose from cryptic splicing of a full-length *neo* message to exon 6 of *u-PAR*. The presence of the *neo* STOP codon as revealed by cycle-sequencing, ensures however termination of translation at this site and excludes the expression of a neo/u-PAR-domain 3 fusion protein.

Absence of u-PAR antigen from the surface of *u-PAR*$^{-/-}$ cells was confirmed in an ELISA assay on coated embryonic fibroblast cells using a polyclonal rabbit anti–murine u-PAR antibody. Absence of functional receptor in *u-PAR*$^{-/-}$ mice was demonstrated by the lack of specific binding of an amino-terminal fragment of murine u-PA (containing amino acid residues 1 to 48) to cultured thioglycollate-stimulated *u-PAR*$^{-/-}$ macrophages. Indeed, binding of radiolabeled ligand to *u-PAR*$^{-/-}$ macrophages was $< 2\%$ of the value obtained with *u-PAR*$^{+/+}$ macrophages and comparable to the background binding to *u-PAR* $^{+/+}$ or *u-PAR*$^{+/-}$ cells. Gene dose-dependent expression of u-PAR was observed in the binding assay as well as in the ELISA, as illustrated by the intermediate behavior of *u-PAR*$^{+/-}$ cells as compared to *u-PAR*$^{+/+}$ and *u-PAR*$^{-/-}$ cells.

u-PAR–deficiency did not compromise embryonic development and viability of the mice, in accordance with previous observations on mice deficient for other components of the fibrinolytic system including u-PA and/or t-PA (16), plasminogen (34), and the inhibitors plasminogen activator inhibitor type-1 (23) or α_2-macroglobulin (35), and implying a less essential role for the plasminogen activation system and u-PA/u-PAR in embryo implantation, development, and viability than previously assumed (36). *u-PAR*$^{-/-}$ mice displayed normal growth and fertility, and no histological abnormalities were found in tissues from 4.5-wk-old mice. *u-PAR*$^{-/-}$ mice did not differ from wild-type mice for spontaneous lysis of an experimental normal murine plasma clot. This finding confirmed our previous observations obtained in u-PA–deficient mice (16) and supports the notion that u-PA has only a minor contribution to endogenous thrombolysis.

The u-PA receptor has been proposed to provide a mechanism for concentrating u-PA activity at cell surfaces, thereby allowing, directly or indirectly via plasmin generation, localized matrix degradation and invasion of migratory cells through anatomical barriers and into tissues (2-4). No difference in numbers of cells invading into the peritoneal cavity upon thioglycollate injection was observed between *u-PAR*$^{+/+}$, *u-PAR*$^{+/-}$, and *u-PAR*$^{-/-}$ mice. However, macrophages from *u-PAR*$^{-/-}$ mice indeed displayed reduced u-PA–mediated plasminogen activating potential at time points up to 3 h which can be explained by the absence of endogenous cell-bound u-PA on the receptor-deficient cells. The observation that at later time points plasminogen activation by *u-PAR*$^{-/-}$ macrophages was similar to that by *u-PAR*$^{+/+}$ macrophages might be explained by an increased contribution by u-PA accumulating in the medium. Control experiments with the u-PA inhibitor amiloride and with stimulators of t-PA activity (CNBr fragments of fibrinogen) indicated that plasmin generation in the assay was indeed u-PA mediated. Macrophages from u-PA–deficient mice have previously been shown to have an impaired capacity for in vitro degradation of extracellular matrices (16). However, macrophages from the present *u-PAR*$^{-/-}$ mice degraded matrices at a similar rate as *u-PAR*$^{+/+}$ macrophages. This again might be explained by the action of u-PA secreted in the medium during the assay. In addition, the contribution of plasminogen-independent proteolytic activity might obscure possible differences between the u-PAR–deficient and wild-type genotypes. Taken together, these findings confirm that the u-PA/u-PAR system represents a mechanism for providing cells with surface-associated proteolytic activity. Nevertheless, u-PAR–deficient macrophages are still capable of invading the peritoneal cavity and are able to degrade extracellular matrix in the experimental conditions described above. The limited phenotype of u-PAR deficiency as analyzed so far suggests that the u-PA/u-PAR system might have a less important contribution to cell-associated proteolytic activity in vivo than generally assumed or that other systems are able to compensate for the deficiency. Whether cellular distribution of receptor-bound u-PA, local regulation of cell-surface levels of u-PA via u-PAR/LDL-receptor related protein–mediated clearance of u-PA/inhibitor complexes (11, 37), and u-PAR–mediated signal transduction are impaired by *u-PAR* gene inactivation remains to be studied.

In conclusion, homozygous u-PAR–deficient mice generated in this study were viable, healthy, and fertile. *u-PAR* gene inactivation abolished binding of murine u-PA to stimulated peritoneal macrophages and reduced their u-PA–dependent plasminogen activating capacity. These u-PAR–deficient mice may represent a valuable model to study the role of the u-PA/u-PAR system in biological processes requiring extracellular proteolysis, and in ligand-induced signal transduction.

Acknowledgments

The authors wish to thank V. Beelen, E. Demarsin, I. Engelborghs, T. Vancoetsem, B. Van Hoef, and S. Wyns for excellent technical assistance. The authors are grateful to F. Blasi (A.S. Raffaele Scientific Institute, Milan, Italy) for providing the polyclonal anti–murine u-PAR antibody, and to H.Y. Min (Chiron Corporation, Emeryville, CA) for providing the murine u-PA aminoterminal fragment mu-PA.1-48.

This work was supported by National Institutes of Health grant HL-41484.

References

1. Vassalli, J.D., D. Baccino, and D. Belin. 1985. A cellular binding site for the M_r 55,000 form of the human plasminogen activator, urokinase. *J. Cell Biol.* 100:86–92.

2. Vassalli, J.D. 1994. The urokinase receptor. *Fibrinolysis.* 8(Suppl. 1):172–181.

3. Blasi, F., M. Conese, L.B. Møller, N. Pedersen, U. Cavallaro, M.V. Cubellis, F. Fazioli, L. Hernandez-Marrero, P. Limongi, P. Muñoz-Canoves, M. Resnati, et al. 1994. The urokinase receptor: structure, regulation and inhibitor-mediated internalization. *Fibrinolysis.* 8 (Suppl. 1):182–188.

4. Danø, K., N. Behrendt, N. Brünner, V. Ellis, M. Ploug, and C. Pyke.

1994. The urokinase receptor. Protein structure and role in plasminogen activation and cancer invasion. *Fibrinolysis.* 8(Suppl 1):189–203.

5. Estreicher, A., J. Mülhauser, J.L. Carpentier, L. Orci, and J.D. Vassalli. 1990. The receptor for urokinase type plasminogen activator polarizes expression of the protease to the leading edge of migrating monocytes and promotes degradation of enzyme inhibitor complexes. *J. Cell Biol.* 111:783–792.

6. Rømer, J., L.R. Lund, J. Eriksen, C. Pyke, P. Kristensen, and K. Danø. 1994. The receptor for urokinase-type plasminogen activator is expressed by keratinocytes at the leading edge during re-epithelialization of mouse skin wounds. *J. Invest. Dermatol.* 102:519–522.

7. Blasi, F., J.D. Vassalli, and K. Danø. 1987. Urokinase-type plasminogen activator: proenzyme, receptor and inhibitors. *J. Cell Biol.* 104:801–804.

8. Plough, M., E. Rønne, N. Behrendt, A.L. Jensen, F. Blasi, and K. Danø. 1991. Cellular receptor for urokinase plasminogen activator: carboxyl-terminal processing and membrane anchoring by glycosyl-phosphatidylinositol. *J. Biol. Chem.* 266:1926–1933.

9. Solberg, H., D. Lober, J. Eriksen, M. Ploug, E. Rønne, N. Behrendt, K. Danø, and G. Høyer-Hansen. 1992. Identification and characterization of the murine cell surface receptor for the urokinase-type plasminogen activator. *Eur. J. Biochem.* 205:451–458.

10. Behrendt, N., M. Plough, L. Patthy, G. Houen, F. Blasi, and K. Danø. 1991. The ligand-binding domain of the cell surface receptor for urokinase-type plasminogen activator. *J. Biol. Chem.* 266:7842–7847.

11. Cubellis, M.V., T.C. Wun, and F. Blasi. 1990. Receptor-mediated internalization and degradation of urokinase is caused by its specific inhibitor PAI-1. *EMBO J.* 9:1079–1085.

12. Olson, D., J. Pöllänen, G. Høyer-Hansen, E. Rønne, K. Sakaguchi, T.C. Wun, E. Appella, K. Danø, and F. Blasi. 1992. Internalization of the urokinase-plasminogen activator inhibitor type-1 complex is mediated by the urokinase receptor. *J. Biol. Chem.* 267:9129–9133.

13. Nusrat, A.R., and H.A. Chapman, Jr. 1991. An autocrine role for urokinase in phorbol ester–mediated differentiation of myeloid cell lines. *J. Clin. Invest.* 87:1091–1097.

14. Rabbani, S.A., A.P. Mazar, S.M. Bernier, M. Haq, I. Bolivar, J. Henkin, and D. Goltzman. 1992. Structural requirements for the growth factor activity of the amino-terminal domain of urokinase. *J. Biol. Chem.* 267:14151–14156.

15. Anichini, E., G. Fibbi, M. Pucci, R. Caldini, M. Chevanne, and M. Del Rosso. 1994. Production of second messengers following chemotactic and mitogenic urokinase-receptor interaction in human fibroblasts and mouse fibroblasts transfected with human urokinase receptor. *Exp. Cell Res.* 213:438–448.

16. Carmeliet, P., L. Schoonjans, L. Kieckens, B. Ream, J. Degen, R. Bronson, R. De Vos, J.J. van den Oord, D. Collen, and R.C. Mulligan. 1994. Physiological consequences of loss of plasminogen activator gene function in mice. *Nature (Lond.).* 368:419–424.

17. Carmeliet, P., J.M. Stassen, M. De Mol, C. Declercq, A. Bouché, and D. Collen. 1994. Arterial neointima formation after trauma in mice with inactivation of the t-PA, u-PA or PAI-1 genes. *Fibrinolysis.* 8(Suppl. 1):101 (Abstr. 280).

18. Lijnen, H.R., B. Van Hoef, and D. Collen. 1986. Comparative kinetic analysis of the activation of human plasminogen by natural and recombinant single-chain urokinase-type plasminogen activator. *Biochim. Biophys. Acta.* 884:402–408.

19. Tybulewicz, V.L., C.E. Crawford, P.K. Jackson, R.T. Bronson, and R.C. Mulligan. 1991. Neonatal lethality and lymphopenia in mice with a homozygous disruption of the c-abl proto-oncogene. *Cell.* 65:1153–1163.

20. Suh, T.T., C. Nerlov, K. Danø, and J.L. Degen. 1994. The murine urokinase-type plasminogen activator receptor gene. *J. Biol. Chem.* 269:25992–25998.

21. Kristensen, P., J. Eriksen, F. Blasi, and K. Danø. 1991. Two alternatively spliced mouse urokinase receptor mRNAs with different histological localization in the gastrointestinal tract. *J. Cell Biol.* 115:1763–1771.

22. Doetschman, T.C., H. Eistetter, M. Katz, W. Schmidt, and R. Kemler. 1985. The in vitro development of blastocyst-derived embryonic stem cell lines: formation of visceral yolk sac, blood islands and myocardium. *J. Embryol. Exp. Morphol.* 87:27–45.

23. Carmeliet, P., L. Kieckens, L. Schoonjans, B. Ream, A. Van Nuffelen, G. Prendergast, M. Cole, R. Bronson, D. Collen, and R.C. Mulligan. 1993. Plasminogen activator inhibitor-1 gene-deficient mice. I. Generation by homologous recombination and characterization. *J. Clin. Invest.* 92: 2746–2755.

24. Bradley, A. 1987. Production and analysis of chimeric mice. *In* Teratocarcinomas and Embryonic Stem Cells. A Practical Approach. E.J. Robertson, editor. IRL Press, Oxford. 113–151.

25. Sambrook, J., E.F. Fritsch, and T. Maniatis. 1989. Molecular Cloning: A Laboratory Manual. Cold Spring Harbor Laboratory Press, Cold Spring Harbor, New York. 1659.

26. Wurst, W., and A.L. Joyner. 1993. Production of targeted embryonic stem cell clones. *In* Gene Targeting. A Practical Approach. A.L. Joyner, editor. IRL Press, Oxford. 33–61.

27. Stassen, J.M., I. Vanlinthout, H.R. Lijnen, and D. Collen. 1990. A hamster pulmonary embolism model for the evaluation of the thrombolytic and pharmacokinetic properties of thrombolytic agents. *Fibrinolysis.* 4(Suppl 2):15–21.

28. Baker, M.S., P. Bleakley, G.C. Woodrow, and W.F. Doe. 1990. Inhibition of cancer cell urokinase plasminogen activator by its specific inhibitor PAI-2 and subsequent effects on extracellular matrix degradation. *Cancer Res.* 50:4676–4684.

29. Lijnen, H.R., B. Van Hoef, V. Beelen, and D. Collen. 1994. Characterization of the murine plasma fibrinolytic system. *Eur. J. Biochem.* 224:863–871.

30. Appella, E., E.A. Robinson, S.J. Ullrich, M.P. Stoppelli, A. Corti, G. Cassani, and F. Blasi. 1987. The receptor-binding sequence of urokinase. A biological function for the growth-factor module of proteases. *J. Biol. Chem.* 262: 4437–4440.

31. Estreicher, A., A. Wohlwend, D. Belin, W.D. Schleuning, and J.-D. Vassalli. 1989. Characterization of the cellular binding site for the urokinase-type plasminogen activator. *J. Biol. Chem.* 264:1180–1189.

32. Unkeless, J.C., S. Gordon, and E. Reich. 1974. Secretion of plasminogen activator by stimulated macrophages. *J. Exp. Med.* 139:834–850.

33. Høyer-Hansen, G., E. Rønne, H. Solberg, N. Behrendt, M. Ploug, L.R. Lund, V. Ellis, and K. Danø. 1992. Urokinase plasminogen activator cleaves its cell surface receptor releasing the ligand-binding domain. *J. Biol. Chem.* 267: 18224–18229.

34. Ploplis, V.A., P. Carmeliet, S. Vazirzadeh, I. Van Vlaenderen, L. Moons, E.F. Plow, and D. Collen. 1995. Effects of disruption of the plasminogen gene in mice on thrombosis, growth and health. *Circulation.* 92:2585–2593.

35. Umans, L., L. Serneels, L. Overbergh, K. Lorent, F. Van Leuven, and H. Van den Berghe. 1995. Targeted inactivation of the mouse α_2-macroglobulin gene. *J. Biol. Chem.* 270:19778–19785.

36. Herz, J., D.E. Clouthier, and R.E. Hammer. 1992. LDL receptor-related protein internalizes and degrades uPA-PAI-1 complexes and is essential for embryo implantation. *Cell.* 71:411–421.

37. Nykjaer, A., C.M. Petersen, B. Møller, P.A. Jensen, S.K. Moestrup, T.L. Holtet, M. Etzerodt, H.C. Thogersen, M. Munch, P.A. Andreasen, and J. Gliemann. 1992. Purified α_2-macroglobulin receptor/LDL receptor-related protein binds urokinase-plasminogen activator inhibitor type-1 complex. Evidence that the α_2-macroglobulin receptor mediates cellular degradation of urokinase receptor-bound complexes. *J. Biol. Chem.* 267:14543–14546.